An experimental study of the reactivity and relative basicity of the methoxide anion in the gas phase at room temperature, and their perturbation by methanol solvation

GERVASE I. MACKAY, ASIT B. RAKSHIT, AND DIETHARD K. BOHME

Department of Chemistry and Centre for Research in Experimental Space Science, York University, Downsview, Ont., Canada M3J 1P3

Received January 19, 1982

GERVASE I. MACKAY, ASIT B. RAKSHIT, and DIETHARD K. BOHME. Can. J. Chem. 60, 2594 (1982).

Flowing afterglow measurements at 296 ± 2 K are reported which explore three aspects of the gas-phase acid–base chemistry of the methoxide anion. Firstly, the intrinsic reactivity of this ion has been determined from measurements of rate constants for solvent-free proton-transfer reactions with molecules more acidic than methanol including $CH_2{=}C{=}CH_2$, $C_6H_5CH_3$, C_2H_5OH, C_2H_2, CH_3CN, CH_3COCH_3, CH_3CHO, CH_3NO_2, and HCN. Secondly, equilibrium constant measurements have been performed for solvent-free proton-transfer reactions which provide a gas-phase scale of acidities for these molecules relative to the acidity of methanol. Finally, rate constants were measured for the reactions of these acids with methoxide ions solvated with up to three molecules of methanol. The results establish trends in reactivity as a function of step-wise solvation when relative acidity is preserved and when a reversal occurs in the relative acidity upon solvation.

GERVASE I. MACKAY, ASIT B. RAKSHIT et DIETHARD K. BOHME. Can. J. Chem. 60, 2594 (1982).

On rapporte les mesures d'écoulement après incandescence à 296 ± 2 K qui explorent trois aspects de la chimie acide–base en phase gazeuse de l'anion méthanolate. Premièrement, on a déterminé la réactivité intrinsèque de cet ion à partir des mesures des constantes de vitesse de réactions de transfert de proton libre du solvant avec les molécules plus acides que le méthanol incluant: $CH_2{=}C{=}CH_2$, $C_6H_5CH_3$, C_2H_5OH, C_2H_2, CH_3COCH_3, CH_3CHO, CH_3NO_2 et HCN. Deuxièment, on a mesuré la constante d'équilibre des réactions de transfert de proton libre du solvant qui fournissent une échelle d'acidité en phase gazeuse de ces molécules par rapport à l'acidité du méthanol. Finalement, on a mesuré les constantes de vitesse des réactions de ces acides avec les ions méthanolates solvatés par un maximum de trois molécules de méthanol. Les résultats établissent les tendances de réactivité en fonction d'une solvatation par étape lorsque l'acidité relative est préservée et quand il se produit une inversion dans l'acidité relative lors de la solvatation.

[Traduit par le journal]

Introduction

Recent studies of gas-phase reactions of anions which have solution analogues have provided, for the first time, a direct quantitative measure of the *intrinsic* stability and reactivity of anions found in solution and an assessment of the absolute influence of solvation on these quantities. For example, gas-phase measurements of rate and equilibrium constants for solvent-free acid–base reactions of type [1]

$$[1]\quad B^- + AH \rightleftharpoons A^- + BH$$

and solvated acid–base reactions of type [2]

$$[2]\quad B^-.S_n + AH \rightleftharpoons A^-.S_n + BH$$

have provided both a measure of the absolute intrinsic reactivity and relative intrinsic basicity of anions as well as an indication of their perturbation by step-wise solvation. This has been illustrated by results obtained recently in our laboratory using the flowing afterglow technique for reactions of the hydroxide ion, an important base in solution (1, 2). Here we report an extension of our studies to the acid–base chemistry of the methoxide ion. Three aspects of this chemistry have been explored. Firstly, the intrinsic reactivity of the methoxide ion has been determined from measurements of rate constants for solvent-free proton-transfer reactions with molecules more acidic than methanol in the gas phase. Secondly, equilibrium constant measurements have been carried out for solvent-free proton-transfer reactions to provide a gas-phase scale of acidities of acids relative to the acidity of methanol. Finally, experiments were performed with methoxide ions solvated with up to three added methanol molecules which provide insight into the perturbation of the intrinsic reactivity and basicity of the methoxide ions by step-wise methanol solvation. The reagent acids were chosen to cover a range in overall energetics sufficient to establish the pattern of this perturbation which appeared to emerge from these studies.

Experimental

The experiments were performed in a flowing plasma mass spectrometer (flowing afterglow) system. Details of the instrument together with the method of operation and data analysis have been elaborated elsewhere (3, 4). The anions were produced in a flowing plasma either by electron impact or by secondary ionization or ion–molecule reactions and were permitted to thermalize by collisions with a helium or hydrogen buffer gas to the ambient room temperature of 296 ± 2 K prior to entering the reaction region. The plasma was generated with ionizing electrons having energies in the range 35–70 eV. The filament emission of the electron gun was maintained at a fixed

0008-4042/82/202594-12$01.00/0

TABLE 1. Rate and equilibrium constants measured for proton-transfer reactions of solvent-free anions at 296 ± 2 K

Reaction	k^a	K^b
$CH_3O^- + H_2CCCH_2 \rightarrow H_2CCCH^- + CH_3OH$	0.87±0.35	1.4±0.3
$CH_3O^- + C_6H_5CH_3 \rightarrow C_6H_5CH_2^- + CH_3OH$	1.5±0.5	1.4±0.3
$CH_3O^- + C_2H_5OH \rightarrow C_2H_5O^- + CH_3OH$	3.3±1.0	
$CH_3O^- + C_2H_2 \rightarrow C_2H^- + CH_3OH$	1.6±0.4	$(2.7\pm0.7)\times 10^3$
$CH_3O^- + CH_3CN \rightarrow CH_2CN^- + CH_3OH$	3.5±0.9	$\geq 1\times 10^4$
$CH_3O^- + CH_3COCH_3 \rightarrow CH_3COCH_2^- + CH_3OH$	2.3±0.6	$\geq 1\times 10^4$
$CH_3O^- + CH_3CHO \rightarrow {}^-CH_2CHO + CH_3OH$	2.0±0.6	$\geq 1\times 10^4$
$CH_3O^- + CH_3NO_2 \rightarrow CH_2NO_2^- + CH_3OH$	3.1±0.8	$\geq 1\times 10^4$
$CH_3O^- + HCN \rightarrow CN^- + CH_3OH$	3.3±0.8	$\geq 1\times 10^4$
$H_2CCCH^- + C_2H_2 \rightarrow C_2H^- + H_2CCCH_2$	0.70±0.18	$(2.1\pm0.5)\times 10^3$
$C_2H_5O^- + C_2H_2 \rightarrow C_2H^- + C_2H_5OH$	1.4±0.4	17±4
$(CH_3)_2CHO^- + C_2H_2 \rightarrow C_2H^- + (CH_3)_2CHOH$	≥0.1	1.2±0.3
$C_2H^- + CH_3CN \rightarrow CH_2CN^- + C_2H_2$	1.5±0.4	$(3.0\pm0.7)\times 10^2$
$CH_2CN^- + CH_3COCH_3 \rightarrow CH_3COCH_2^- + CH_3CN$	0.30±0.09	$\geq 5\times 10^2$

[a] The measured forward rate constant along with the estimated uncertainty in units of 10^{-9} cm^3 molecule^{-1} s^{-1}.

[b] The value of K represents the weighted mean together with its standard error of measurements including one or more of k_f/k_r and K_{ratio} in one or both directions of reaction.

TABLE 2. Rate constants[a] measured for reactions of solvated methoxide ions with acids, AH, in the gas phase at 296 ± 2 K

AH	$CH_3O^-.CH_3OH$	$CH_3O^-.(CH_3OH)_2$	$CH_3O^-.(CH_3OH)_3$
H_2CCCH_2	≤ 0.001	≤ 0.001	≤ 0.001
CH_3CCH	≤ 0.001		
$C_6H_5CH_3$	≤ 0.001		
C_2H_5OH	2.9±1.0	1.2±0.4	≥ 0.2
C_2H_2	≤ 0.001		
CH_3CN	≤ 0.001	≤ 0.002	≤ 0.002
CH_3COCH_3	1.7±0.4	≤ 0.002	≤ 0.002
CH_3CHO	1.5±0.6	≤ 0.01	≤ 0.01
CH_3NO_2	2.3±0.7	1.9±0.6	1.3±0.5
HCN	3.2±1.0	3.1±1.0	3.0±1.1

[a] Rate constants and their estimated accuracies are given in units of 10^{-9} cm^3 molecule^{-1} s^{-1}.

value in the range 0.5 to 1.5 mA. The ions present in the plasma were sampled through a small orifice mounted at the tip of a nose cone situated at the end of the reaction region and mass analysed with a quadrupole mass spectrometer. The observed variation in the ion signals as a function of neutral reagent addition provided the raw data from which the rate and equilibrium constants were determined. As has been the case in our previous studies, the buffer, source, and reagent gases or vapours were all of high purity.

Methoxide ions were generated by passing CH_3OH into a He or H_2 buffer gas upstream of the filament at total pressures of ca. 0.4 Torr. The ions were solvated by reactions of type [3].

$$[3] \quad CH_3O^-.(CH_3OH)_n + CH_3OH + He(H_2) \rightarrow CH_3O^-.(CH_3OH)_{n+1} + He(H_2)$$

The partial pressure of methanol was varied from ca. 0.005 to 2 mTorr in order to change the initial relative population of the cluster ions $CH_3O^-.(CH_3OH)_n$; n was observed to take on values between 0 and 3 at the operating conditions of the experiments reported here. In deriving rate constants from the observed decays of $CH_3O^-.(CH_3OH)_n$, account was taken of the initial decay which could arise due to the depletion of the precursor ion $CH_3O^-.(CH_3OH)_{n-1}$. The magnitude of this depletion could be assessed in those studies in which the daughter ion $CH_3O^-.(CH_3OH)_n$ did not react with the added neutral reagent.

Results

The rate and equilibrium constants measured in this study for acid–base reactions of types [1] and [2] are summarized in Tables 1 and 2. The sources of uncertainty have been described previously (3, 4). The following section provides a more detailed account of the measurements. They are presented in order of increasing acidity of the reagent acid.

H_2CCCH_2

CH_3O^- was established in both He and H_2 carrier gases at low methanol flows and moderately low pressures to avoid significant depletion of CH_3O^- by clustering. Under these conditions the dominant source and sink of CH_3O^- in the reaction region upon the addition of allene was the reversible reaction:

$$[4] \quad CH_3O^- + H_2CCCH_2 \rightleftharpoons H_2CCCH^- + CH_3OH$$

We have reported elsewhere that the deprotonation of allene in this fashion is expected to establish the allenyl anion without subsequent 1,3-hydrogen migration to form the isomeric $CH_3—C≡C^-$ structure (5). A minor product (< 1%) of unknown origin was observed at $m/e = 38$ ($C_3H_2^-$?) but it was sufficiently small to be ignored in the equilibrium analysis. The experiments provided values for $k_4 = (8.7 \pm 3.5) \times 10^{-10}$ cm³ molecule⁻¹ s⁻¹, $k_4/k_{-4} = 1.36 \pm 0.41$ and $K_4 = 1.40 \pm 0.42$. The $CH_3O^-.CH_3OH$ in the reaction region did not react with allene, $k \leq 1 \times 10^{-12}$ cm³ molecule⁻¹ s⁻¹. An extended analysis of the data confirmed that its presence did not prevent the determination of a reliable value for the true equilibrium constant of reaction [4]. Doubly and triply solvated methoxide ions were established at higher flows of methanol and these also did not react with allene.

One investigation was carried out in an attempt to determine the equilibrium constant for reaction [4] from the reverse direction. The H_2CCCH^- ions were produced by proton transfer to OH^- prior to the reaction region. At low additions of methanol the CH_3O^- signal was observed to increase rapidly with an accompanying decline in the H_2CCCH^- signal, indicating that proton transfer to H_2CCCH^- from methanol is rapid and the major loss process for H_2CCCH^- in the reaction region. The CH_3O^- was observed to decline at large additions of methanol as a result of clustering. It was possible to fit the variations in the H_2CCCH^- and CH_3O^- signals using an extended analysis by incorporating the value for $k_4/k_{-4} = 1.36$ obtained from the forward study and a value of $k = 9.3 \times 10^{-27}$ cm⁶ molecule⁻² s⁻¹ for the three-body rate constant of clustering determined from the decay of the CH_3O^- signal at large methanol additions. This result provides additional confidence in the value of the equilibrium constant determined from the study in the forward direction.

The proton-transfer equilibrium

$$[5] \quad H_2CCCH^- + C_2H_2 \rightleftharpoons C_2H^- + H_2CCCH_2$$

was investigated with the addition of acetylene into a He (or H_2) – H_2CCCH_2 – H_2O plasma in which H_2CCCH^- is produced initially by proton transfer from allene to OH^- or directly by electron impact on allene. Small but negligible amounts of an ion at $m/e = 38$ were again observed to be produced. Analysis of the observed decay of the H_2CCCH^- ion provided values for $k_5 = (7.0 \pm 1.8) \times 10^{-10}$ cm³ molecule⁻¹ s⁻¹ and $k_5/k_{-5} = (2.1 \pm 0.6) \times 10^3$. The ion signal ratio plots at high additions of C_2H_2 provided a value for $K_5 = (2.3 \pm 0.8) \times 10^3$. The flow of allene was varied from 2.17×10^{17} to 2.4×10^{19} molecules s⁻¹. No attempt was made to investigate this equilibrium from the reverse direction due to the large value of the equilibrium constant.

CH_3CCH

Figure 1 shows the variation of the dominant negative ions resulting from the addition of propyne into a He–CH_3OH plasma in which CH_3O^- is initially a dominant negative ion. $C_3H_3^-$ is rapidly produced by the reaction

$$[6] \quad CH_3O^- + CH_3CCH \rightarrow C_3H_3^- + CH_3OH$$

and it reacts further with propyne to produce C_2H^-, presumably by the nucleophilic-displacement reaction:

$$[7] \quad C_3H_3^- + CH_3CCH \rightarrow C_2H^- + C_4H_6$$

Some production of C_2H^- from the direct displacement by CH_3O^- could not be excluded. The impurity ion Cl^- and the cluster ion $CH_3O^-.CH_3OH$ are seen to be insensitive to the addition of propyne.

The deprotonation of propyne in reaction [6] may proceed either at the methyl or acetylenyl positions. The former will lead to an anion which rearranges to the allenyl anion (5):

$$[8] \quad {}^-CH_2—C≡CH \rightarrow CH_2=C=CH^-$$

Further rearrangement to the more stable $CH_3—C≡C^-$ anion by 1,3-hydrogen migration involves a large activation barrier (6). Separate measurements have shown that deprotonation of propyne by OH^- occurs predominantly at the methyl position so that most of the $C_3H_3^-$ produced in reaction [6] can be expected to be of the allenyl form. This implies that the reaction which introduces the observed curvature in the decay of CH_3O^- is likely to be:

$$[9] \quad C_3H_3^- + CH_3OH \rightarrow CH_3O^- + CH_2=C=CH_2$$

rather than the true reverse to reaction [6] which would regenerate propyne.

Reaction [7] was investigated separately in experiments in which $C_3H_3^-$ was produced from either allene or propyne by deprotonation with OH^- (5). The measured rate constant was observed to be insensitive to the history of $C_3H_3^-$ and to have a value of $(8.0 \pm 2.0) \times 10^{-11}$ cm³ molecule⁻¹ s⁻¹.

$C_6H_5CH_3$

The study of reaction [10] was straightforward.

$$[10] \quad CH_3O^- + C_6H_5CH_3 \rightleftharpoons C_6H_5CH_2^- + CH_3OH$$

Proton transfer was the only observed product channel proceeding with a rate constant of $(1.5 \pm 0.5) \times 10^{-9}$ cm³ molecule⁻¹ s⁻¹. The cluster ion $CH_3O^-.CH_3OH$ was observed not to react rapidly with toluene, $k \leq 10^{-12}$ cm³ molecule⁻¹ s⁻¹. No

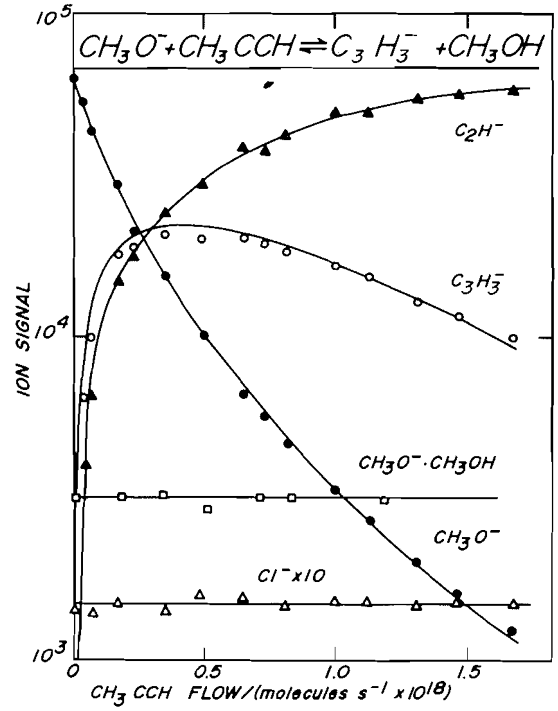

FIG. 1. The variation in dominant negative ions observed upon the addition of propyne into a He–CH_3OH plasma in which CH_3O^- is initially a dominant negative ion. $T = 296\,K$, $P = 0.354$ Torr, $\bar{v} = 7.7 \times 10^3$ cm s^{-1}, $L = 59$ cm, and the CH_3OH flow is 2.0×10^{17} molecules s^{-1}.

evidence was found for competing and/or secondary reactions involving $C_6H_5CH_2^-$. Analysis of the observed CH_3O^- decays under conditions approaching equilibrium provided a value for $k_{10}/k_{-10} = 1.4 \pm 0.5$ which is in exact agreement with the value for $K_{10} = 1.4 \pm 0.5$ obtained from ratio plot analyses under equilibrium conditions. Equilibrium was also approached from the reverse direction for which $C_6H_5CH_2^-$ was produced from the proton transfer between OH^- and toluene. The decay of this ion at low methanol flows provided a value for $k_{10}/k_{-10} = 1.3 \pm 0.6$ while the equilibrium ion ratio led to a value for $K_{10} = 1.2 \pm 0.5$.

C_2H_5OH

The decays in the ion signals corresponding to CH_3O^- and the solvated ions $CH_3O^-.CH_3OH$, $CH_3O^-.(CH_3OH)_2$, and $CH_3O^-.(CH_3OH)_3$ observed upon the addition of ethanol into a He–CH_3OH plasma are shown in Fig. 2. Analysis of the data indicated that all of these ions react rapidly with ethanol in solvated acid–base reactions of type [11] with rate constants of (3.3 ± 1.0), (2.9 ± 1.0), (1.2 ± 0.4), and $(>0.2) \times 10^{-9}$ cm^3 molecule^{-1} s^{-1}, respectively.

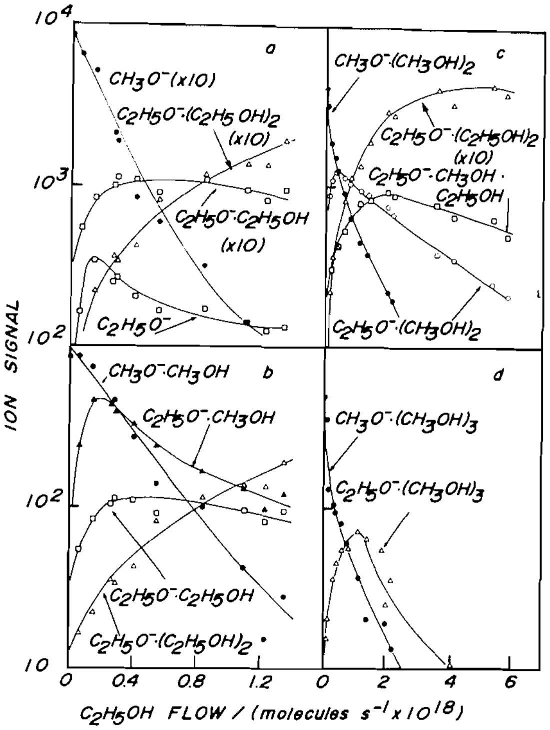

FIG. 2. A split view of observations recorded for the reactions of $CH_3O^-.(CH_3OH)_n$ with ethanol. The buffer gas is He. $T = 295\,K$, $P = 0.333$ Torr, $\bar{v} = 8.1 \times 10^3$ cm s^{-1}, $L = 46$ cm, and the methanol flow is approximately 6×10^{19} molecules s^{-1}.

$$[11] \quad CH_3O^-.(CH_3OH)_n + C_2H_5OH \rightarrow C_2H_5O^-.(CH_3OH)_n + CH_3OH$$

The product ions $C_2H_5O^-.(CH_3OH)_n$ at $n = 0$ to 3 were observed to rise and then fall in concentration indicating further rapid reactions with ethanol. Evidently solvent exchange or "switching" reactions of type [12] were occurring.

$$[12] \quad C_2H_5O^-.(CH_3OH)_n + C_2H_5OH \rightarrow C_2H_5O^-.(CH_3OH)_{n-1}.C_2H_5OH + CH_3OH$$

Both $C_2H_5O^-.C_2H_5OH$ and $C_2H_5O^-.CH_3OH.$-C_2H_5OH were observed to rise concomitant to the fall of the corresponding $C_2H_5O^-.(CH_3OH)_n$ species. $C_2H_5O^-.CH_3OH.C_2H_5OH$ was observed to displace still another methanol molecule according to reaction [13].

$$[13] \quad C_2H_5O^-.CH_3OH.C_2H_5OH + C_2H_5OH \rightarrow C_2H_5O^-.(C_2H_5OH)_2 + CH_3OH$$

Finally, the profiles in Fig. 2 also provide evidence for the occurrence of ethanol addition reactions of type [14] for $n = 0$ and 1.

$$[14] \quad C_2H_5O^-.(C_2H_5OH)_n + C_2H_5OH + He \rightarrow C_2H_5O^-.(C_2H_5OH)_{n+1} + He$$

Taken together, the solvated proton-transfer reactions of type [11] appear to indicate sequences of solvent switching and solvent addition reactions which combine to ultimately establish the ethoxide ion solvated exclusively by ethanol.

While the unsolvated proton-transfer reaction between CH_3O^- and C_2H_5OH did not appear to attain equilibrium under our operating conditions, an analysis of the dependence on ethanol flow of the solvated product to reactant ion ratios for reactions of type [11] for $n = 1, 2$, and 3 did indicate regimes of methanol and ethanol flow for which equilibrium appeared to be established. Figure 3 shows the attainment of equilibrium for the solvated proton-transfer reaction [15] as well as the

[15] $$CH_3O^-.CH_3OH + C_2H_5OH \rightleftharpoons C_2H_5O^-.CH_3OH + CH_3OH$$

ensuing solvent-switching reaction [16]. The linearity observed in the ion ratio plots for these

[16] $$C_2H_5O^-.CH_3OH + C_2H_5OH \rightleftharpoons C_2H_5O^-.C_2H_5OH + CH_3OH$$

two reactions provided values for K of 7.6 ± 2.7 and 2.0 ± 1.0, respectively. For the higher solvated proton-transfer reactions of type [11] with $n = 2$ and 3, an analysis of the data indicated values for the equilibrium constants of approximately 4 and 1, respectively.

An unsuccessful attempt was made to approach equilibrium for the unsolvated proton-transfer reaction from its reverse direction by adding methanol into a He–C_2H_5OH plasma in which $C_2H_5O^-$ was initially a dominant negative ion. However, equilibrium was again observed to be established for reactions [15] and [16]. The equilibrium constants deduced from the corresponding ratio plots were in good agreement with those derived from the forward study having values of 7.8 ± 3.9 and 2.5 ± 0.9, respectively.

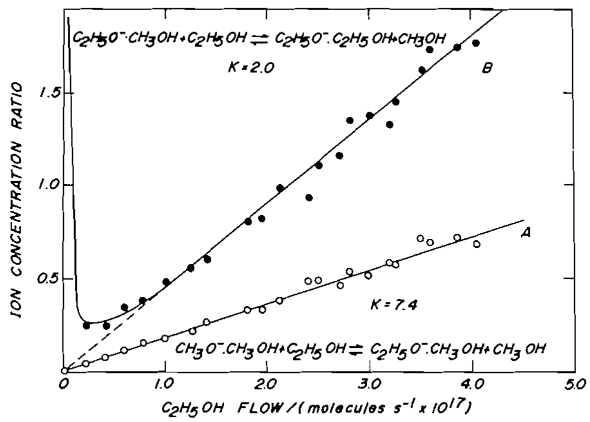

FIG. 3. The variation in ion concentration ratios observed upon the addition of ethanol into a He–CH_3OH plasma. T = 295 K, P = 0.354 Torr, $\bar{v} = 8.4 \times 10^3$ cm s^{-1}, L = 85 cm, and the flow of methanol is 4.09×10^{17} molecules s^{-1}. Curve A: the ion concentration ratio $[C_2H_5O^-.CH_3OH]/[CH_3O^-.CH_3OH]$ divided by 10. Curve B: the ion concentration ratio $[C_2H_5O^-.C_2H_5OH]/[C_2H_5O^-.CH_3OH]$. The initial curvature arises from the production of $C_2H_5O^-.CH_3OH$ in the reaction region.

C_2H_2

We have observed the proton-transfer reaction of CH_3O^- with acetylene previously; it proceeded rapidly with a rate constant of $(1.6 \pm 0.4) \times 10^{-9}$ cm^3 $molecule^{-1}$ s^{-1} (7) which was reproduced in the present studies. At the methanol flows used in the present experiments sufficient back reaction was introduced to allow the evaluation of the equilibrium constant for reaction [17] both from the ratios of ion and neutral concentrations at

[17] $$CH_3O^- + C_2H_2 \rightleftharpoons C_2H^- + CH_3OH$$

equilibrium and from the ratio of rate constants derived from the decay of CH_3O^- and they were in good agreement. The values obtained were $(2.6 \pm 1.2) \times 10^3$ and $(2.7 \pm 1.1) \times 10^3$, respectively. Figure 4 shows data which provide a measure of the ratio of rate constants. The solvated species

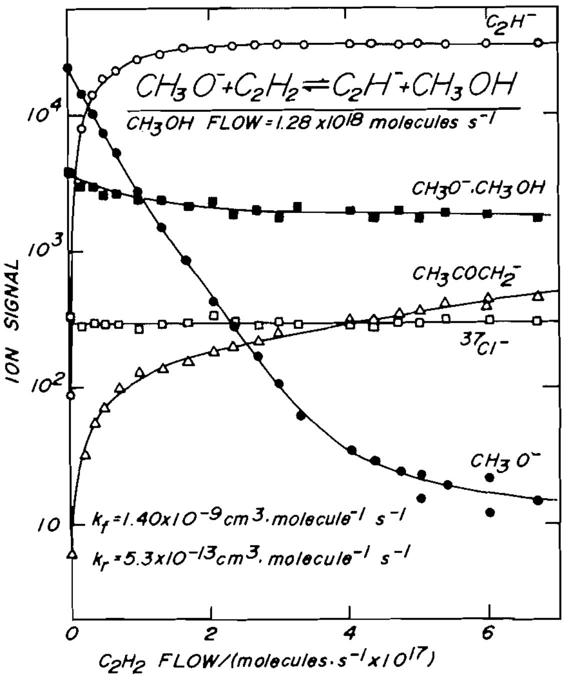

FIG. 4. The variation in dominant negative ions recorded upon the addition of acetylene into a He–CH_3OH plasma in which CH_3O^- is initially a dominant negative ion. The solid line through the CH_3O^- decay represents a computer fit to the data with the values of the rate constants indicated. The initial decay in the $CH_3O^-.CH_3OH$ arises from the depletion of the CH_3O^- source ion. T = 298 K, P = 0.317 Torr, $\bar{v} = 7.7 \times 10^3$ cm s^{-1}, and L = 84 cm.

$CH_3O^-.CH_3OH$ which was also observed to be present in the reaction region, failed to react with a measurable rate, $k \leq 1 \times 10^{-12}$ cm^3 molecule^{-1} s^{-1}.

The reaction of the ethoxide anion

[18] $C_2H_5O^- + C_2H_2 \rightleftharpoons C_2H^- + C_2H_5OH$

could also be driven into equilibrium under quite similar operating conditions. Again there was good agreement between the ratio of rate constants, $k_{18}/k_{-18} = 17.0 \pm 6.8$ and the equilibrium constant derived from equilibrium concentrations, $K_{18} = 16.4 \pm 6.6$. The forward rate constant was determined to be $(1.4 \pm 0.4) \times 10^{-9}$ cm^3 molecule^{-1} s^{-1}. One experiment was carried out in which C_2H^- was produced in a He/CH_4 plasma in the absence of C_2H_2. The rate constant for the reverse reaction, $k_{-18} = 1.0 \times 10^{-10}$ cm^3 molecule^{-1} s^{-1}, could then be evaluated directly from the slope of the C_2H^- decay using Analysis A (3). This value, when coupled with the rate constant obtained from the forward study, provided a value for $k_{18}/k_{-18} = 14 \pm 8$. The cluster ion $C_2H_5O^-.C_2H_5OH$ became the dominant primary ion in the reaction region already at relatively low flows, 2×10^{17} molecules s^{-1}. It was also observed not to react with C_2H_2, $k \leq 1 \times 10^{-12}$ cm^3 molecule^{-1} s^{-1}.

With $(CH_3)_2CHO^-$ equilibrium was established already at the smallest measurable additions of C_2H_2. This precluded the determination of unique values for the forward and reverse rate constants for reaction [19].

[19] $(CH_3)_2CHO^- + C_2H_2 \rightleftharpoons C_2H^- + (CH_3)_2CHOH$

The measurements did, however, provide values for the ratio of rate constants $k_{19}/k_{-19} = 1.16 \pm 0.41$ and the equilibrium constant derived from equilibrium concentrations $K_{19} = 1.13 \pm 0.45$.

CH_3CN

We have reported previously that reaction [20]

[20] $CH_3O^- + CH_3CN \rightarrow CH_2CN^- + CH_3OH$

proceeds very rapidly with a rate constant at room temperature of $(3.5 \pm 0.9) \times 10^{-9}$ cm^3 molecule^{-1} s^{-1} without any significant displacement to form CN^- (8). Furthermore, the reaction could not be driven to equilibrium under our operating conditions. Consequently attempts were made to establish equilibrium for the less exoergic proton-transfer reaction [21]. Both He and H_2 were used as

[21] $C_2H^- + CH_3CN \rightleftharpoons CH_2CN^- + C_2H_2$

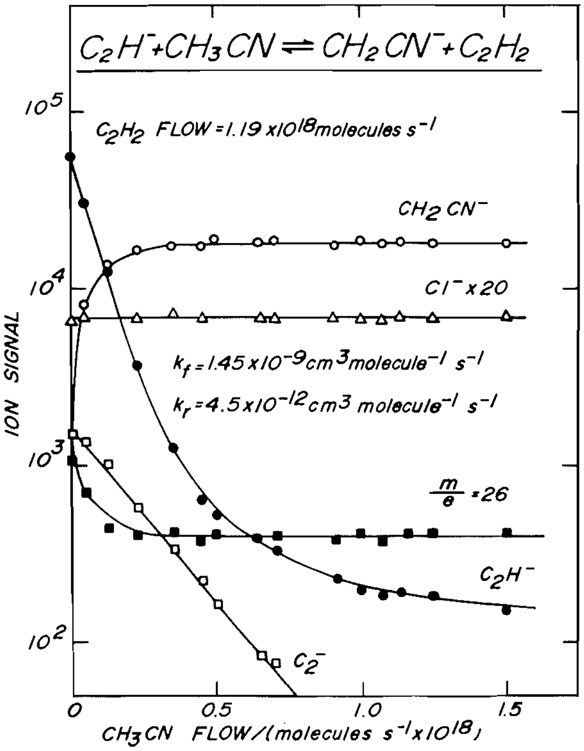

FIG. 5. The variation in dominant negative ions recorded upon the addition of CH_3CN into a He–C_2H_2 plasma in which C_2H^- is initially a dominant negative ion. The solid line through the C_2H^- decay is a computer fit with the values of the rate constants indicated. $T = 295$ K, $P = 0.365$ Torr, $\bar{v} = 8.3 \times 10^3$ cm s^{-1}, and $L = 60$ cm.

buffer gases and the C_2H^- was produced either by electron impact on acetylene at ca. 40 eV or via the rapid proton transfer from C_2H_2 to OH^- (9). Figure 5 shows a representative variation of dominant negative ions recorded upon the addition of acetonitrile into a He–C_2H_2 plasma in which C_2H^- was initially a major ion. The majority of the C_2H^- decay and accompanying increase in the CH_2CN^- signal can be attributed to the proton-transfer reaction [21]. The initial decay in the mass 26 signal is due to the reaction of the $^{13}C^{12}CH^-$ isotope. The failure of the mass 26 ion signal to rise sets an upper limit of 0.5% to the production of CN^- by nucleophilic displacement. The mass discrimination plots in all experiments exhibited excellent linearity over a range in CH_3CN flow which was varied by over a factor of 200 and the mass discrimination factor was found to be independent of the CH_3CN concentration and reaction length which had values of 59 and 85 cm. The application of our standard analyses to the curved C_2H^- decays and the ratio plots led to values for the ratio of rate constants and the equilibrium constant, respectively, which agreed within the uncertainty of the measurements: $k_{21} = (1.5 \pm 0.4) \times 10^{-9}$ and $k_{-21} = (4.8 \pm 1.7) \times 10^{-12}$ cm^3 molecule^{-1} s^{-1}, $k_{21}/k_{-21} = (3.1 \pm 0.9) \times 10^2$, and $K_{21} = (3.0 \pm 1.2) \times 10^2$. The weighted mean of the values for k_{21}/k_{-21} and K_{21}

provides a best estimate of the true value for the equilibrium constant of 3.0 × 10^2 with a standard error of ±0.7 × 10^2 for reaction [21].

The solvated cluster ions $CH_3O^-.(CH_3OH)_n$ with $n = 1$, 2, and 3 were observed not to react rapidly with CH_3CN, $k \leq 2 \times 10^{-12}$ cm^3 $molecule^{-1}$ s^{-1}. Apparently a reversal in the relative acidity of CH_3OH and CH_3CN occurs already at the addition of one solvent methanol molecule.

CH_3COCH_3

Figure 6 shows data which reveal the transition in kinetics with the stepwise solvation of CH_3O^- with methanol in reactions of type [22].

$$[22]\quad CH_3O^-.(CH_3OH)_n + CH_3COCH_3 \rightarrow CH_3COCH_2^-.(CH_3OH)_n + CH_3OH$$

The unsolvated methoxide ion reacts rapidly with a rate constant determined to be (2.3 ± 0.6) × 10^{-9} cm^3 $molecule^{-1}$ s^{-1} but does not approach equilibrium. However, equilibrium was nearly achieved for the reaction of the singly solvated ion for which a slightly smaller rate constant of (1.7 ± 0.4) × 10^{-9} cm^3 $molecule^{-1}$ s^{-1} was obtained, while the doubly and triply solvated species failed to react, $k < 2 \times 10^{-12}$ cm^3 $molecule^{-1}$ s^{-1}.

Since equilibrium could not be established for the solvent-free reaction of the methoxide ion with acetone, an attempt was made to approach an equilibrium in a proton-transfer reaction with the much less basic anion CH_2CN^-. The only product ion formed at low additions of acetone into a He–CH_3CN plasma in which CH_2CN^- was established by proton-transfer from CH_3CN to OH^- was $CH_3COCH_2^-$ so that the decay of CH_2CN^- could be attributed to the proton-transfer reaction [23]. At large acetone additions the clustering reaction [24] proceeded towards equilibrium.

$$[23]\quad CH_2CN^- + CH_3COCH_3 \rightarrow CH_3COCH_2^- + CH_3CN$$

The product to reactant ion concentration ratio at equilibrium provided a value of (1.5 ± 0.5) × 10^6 (standard state = 1 atm) for the equilibrium constant of reaction [24].

$$[24]\quad CH_3COCH_2^- + CH_3COCH_3 + He \rightleftharpoons CH_3COCH_2^-.CH_3COCH_3 + He$$

A small amount of $CH_2CN^-.CH_3CN$ present initially was rapidly depleted by the solvated proton-transfer reaction [25].

$$[25]\quad CH_2CN^-.CH_3CN + CH_3COCH_3 \rightleftharpoons CH_3COCH_2^-.CH_3CN + CH_3CN$$

An extended analysis of the data provided only a lower limit to the equilibrium constant for reaction [23] of 500. The initial decay of CH_2CN^- provided a forward rate constant for reaction [23] of (3.0 ± 0.9) × 10^{-10} cm^3 $molecule^{-1}$ s^{-1}.

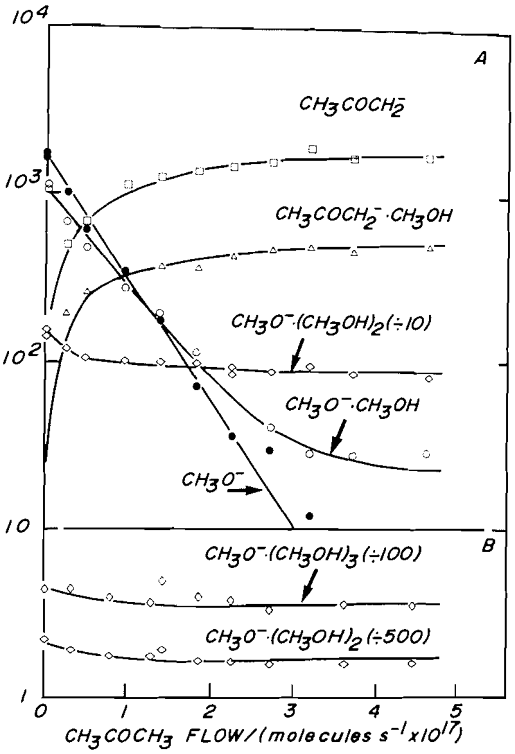

FIG. 6. Observations recorded for the reactions of $CH_3O^-.(CH_3OH)_n$ with acetone in a He buffer at a low flow (*A*: ~5 × 10^{17} molecules s^{-1}) and a high flow (*B*: ~2 × 10^{19} molecules s^{-1}) of methanol. $T = 295$ K, $P = 0.323$ Torr, $\bar{v} = 8 \times 10^3$ cm s^{-1}, and $L = 46$ cm.

An attempt was also made to establish equilibrium for reaction [23] from the reverse direction. It was evident that $CH_3COCH_2^-$ does not react rapidly with CH_3CN either by proton transfer or by CN^- displacement: no significant increase was observed for the m/e = 40 and 26 ion signals. The cluster ion $CH_3COCH_2^-.CH_3CN$ was formed instead by the association reaction [26] for which the ion ratio plot at large flows of CH_3CN indicated an equilibrium constant of (1.0 ± 0.5) × 10^7 (standard state = 1 atm).

$$[26]\quad CH_3COCH_2^- + CH_3CN + He \rightleftharpoons CH_3COCH_2^-.CH_3CN + He$$

Also the solvent-switching reaction [27] appeared to achieve equilibrium with an equilibrium constant of 4 ± 3.

$$[27]\quad CH_3COCH_2^-.CH_3COCH_3 + CH_3CN \rightleftharpoons CH_3COCH_2^-.CH_3CN + CH_3COCH_3$$

CH_3CHO

The solvent-free and singly-solvated methoxide ion were observed to react rapidly with acetaldehyde with rate constants of (2.0 ± 0.6) and (1.5 ± 0.6) × 10^{-9} cm^3 $molecule^{-1}$ s^{-1}. Both $^-CH_2CHO$ and $^-CH_2CHO.CH_3OH$ were observed as product ions in amounts which balanced the initial CH_3O^- and $CH_3O^-.CH_3OH$ signals, respectively, in accordance with reaction [28].

$$[28]\quad CH_3O^-.(CH_3OH)_n + CH_3CHO \rightarrow {}^-CH_2CHO.(CH_3OH)_n + CH_3OH$$

The reactions with $n = 2$ and 3 appeared not to proceed rapidly, $k < 1 \times 10^{-11}$ cm^3 $molecule^{-1}$ s^{-1}, and there was no significant production of $^-CH_2CHO.(CH_3OH)_n$ with $n = 2$ and 3. The $^-CH_2CHO$ reacted further, presumably to form the adduct $^-CH_2CHO.CH_3CHO$ which was observed to appear at larger additions of CH_3CHO into the reaction region. The $^-CH_2CHO.CH_3OH$ appeared to react further by the solvent-switching reaction [29].

$$[29]\quad {}^-CH_2CHO.CH_3OH + CH_3CHO \rightarrow {}^-CH_2CHO.CH_2CHO + CH_3OH$$

CH_3NO_2

The solvent free CH_3O^- and the solvated $CH_3O^-.(CH_3OH)_n$ ions with $n = 1$ to 3 were all observed to react rapidly with nitromethane in reactions of type [30] with rate constants of (3.1 ± 0.8), (2.3 ± 0.7), (1.9 ± 0.6), and (1.3 ± 0.5) × 10^{-9} cm^3 $molecule^{-1}$ s^{-1}, respectively. We have reported previously a rate constant of (3.2 ± 0.8) × 10^{-9} cm^3 $molecule^{-1}$ s^{-1} for the solvent-free reaction (10). All of the corresponding solvated product ions were observed to be produced, albeit $CH_2NO_2^-.(CH_3OH)_3$ appeared in only trace amounts. Also the product ion profiles provided evidence for the exchange of solvent in reactions of type [31] for $n = 1$ and 2, and the addition of CH_3NO_2 to $CH_2NO_2^-$ according to reaction [32]. At the operating conditions of these experiments there was no indication of the establishment of equilibrium in any of the reactions of type [30].

$$[30]\quad CH_3O^-.(CH_3OH)_n + CH_3NO_2 \rightarrow CH_2NO_2^-.(CH_3OH)_m + (n - m + 1)CH_3OH$$

$$[31]\quad CH_2NO_2^-.(CH_3OH)_n + CH_3NO_2 \rightarrow CH_2NO_2^-.CH_3NO_2 + CH_3OH$$

$$[32]\quad CH_2NO_2^- + CH_3NO_2 + He \rightarrow CH_2NO_2^-.CH_3NO_2 + He$$

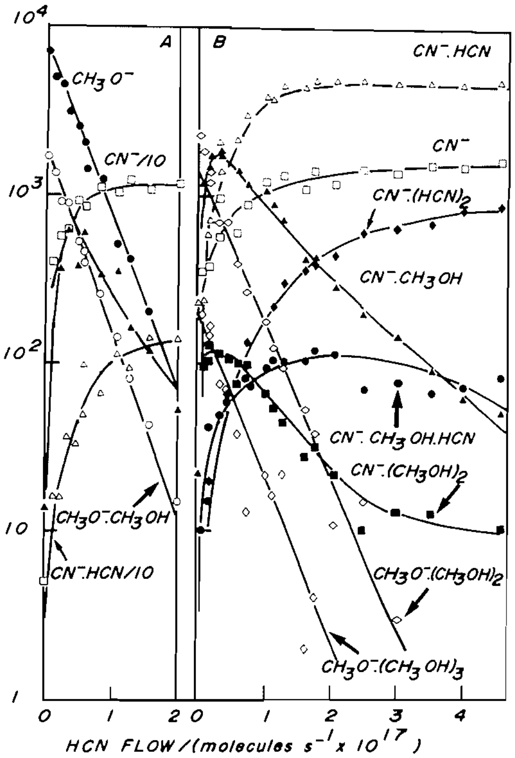

FIG. 7. A split view of observations recorded for the reactions of $CH_3O^-.(CH_3OH)_n$ with hydrogen cyanide at a low flow (*A*: ~1 × 10^{19} molecules s^{-1}) and a high flow (*B*: ~4 × 10^{19} molecules s^{-1}) of methanol. The buffer gas is He. $T = 296$ K, $P = 0.343$ Torr, $\bar{v} = 8.1 \times 10^3$ cm s^{-1}, and $L = 46$ cm.

HCN

Figure 7 reveals the influence of methanol solvation on the reaction of methoxide ion with HCN. Rapid reactions of type [33] were observed for all of the $CH_3O^-.(CH_3OH)_n$ ions with the rate constants for $n = 0, 1, 2$, and 3 having values of (3.3 ± 0.8), (3.2 ± 1.0), (3.1 ± 1.0), and (3.0 ± 1.1) × 10^{-9} cm^3 $molecule^{-1}$ s^{-1}, respectively. The product ion profiles indicated further rapid solvent switching reactions of type [34] for $n = 1$ and 2 for which rate constants of (1.5 ± 0.5) and (1.4 ± 0.5) × 10^{-9} cm^3 $molecule^{-1}$ s^{-1} were deduced. The reaction for $n = 2$ appeared to approach equilibrium (with an equilibrium constant > 1 × 10^3) and was followed by further solvent exchange according to reaction [35] to completely eliminate CH_3OH from the solvation shell of CN^-.

$$[33]\quad CH_3O^-.(CH_3OH)_n + HCN \rightarrow CN^-.(CH_3OH)_m + (n - m + 1)CH_3OH$$

$$[34]\quad CN^-.(CH_3OH)_n + HCN \rightarrow CN^-.(CH_3OH)_{n-1}.HCN + CH_3OH$$

$$[35]\quad CN^-.CH_3OH.HCN + HCN \rightarrow CN^-.(HCN)_2 + CH_3OH$$

Discussion

A. Intrinsic kinetics

The room-temperature rate constants measured in this study for the reactions of solvent-free methoxide anions and several other unsolvated anions are summarized in Table 1. Protonation of the methoxide ion was observed to proceed rapidly in all cases with rate constants exceeding 8 × 10^{-10} cm^3 $molecule^{-1}$ s^{-1}. The corresponding efficiencies determined from the ratios of the measured rate constant to the collision rate constant calculated using the AADO theory (11) all exceed 60%. The slowest and least efficient (10%) reaction measured was that between CH_2CN^- and acetone which involves the protonation of a charge-delocalized anion.

Few other measurements are available for comparison. A rate constant of 6.58 × 10^{-10} cm^3 $molecule^{-1}$ s^{-1}, which is about one-half of our room-temperature value, has been reported for the reaction of CH_3O^- with toluene involving reagent ions with a laboratory energy of ca. 0.3 eV in a tandem spectrometer (12). An ion cyclotron resonance (ICR) measurement of the rate constant for this reaction resulted in a value of only (2.0 ± 0.2) × 10^{-10} cm^3 $molecule^{-1}$ s^{-1} (13) which is about seven times smaller than our value. Better agreement with the ICR results is obtained for the reaction of CH_3O^- with ethanol for which the ICR measurements yielded (1.2 ± 0.3) × 10^{-9} cm^3 $molecule^{-1}$ s^{-1} (13).

Several new association reactions were identified in this study. Of particular note are reaction [24] and the analogous reaction with acetaldehyde. The clustering reactions may also be written as aldol-type condensations as in reaction [36]. Self-condensation reactions of this type are well known in solution where they proceed readily in the presence of aqueous base.

[36] 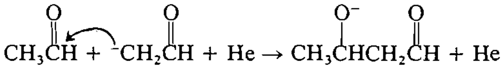

$$\mathrm{CH_3\overset{O}{\overset{\|}{C}}H + {}^{-}CH_2\overset{O}{\overset{\|}{C}}H + He \rightarrow CH_3\overset{O^-}{\overset{|}{C}}HCH_2\overset{O}{\overset{\|}{C}}H + He}$$

B. Intrinsic energetics

Equilibrium constants

The room-temperature equilibrium constants for the solvent-free proton-transfer reactions measured in this study and which provide the basis of the gas-phase scale of acidities derived below are also included in Table 1. The equilibrium constants for the three reactions of alkoxide ions with C_2H_2 supersede those reported a decade ago by Bohme and co-workers (14) in their first attempt to quantify differences in gas-phase acidities of organic compounds. These earlier flowing afterglow measurements, which relied on an inferior method for the measurement of concentrations of alcohol vapours, provided equilibrium constants of 3 × 10, 1 × 10, and 1 for the reactions of CH_3O^-, $C_2H_5O^-$, and $(CH_3)_2CHO^-$, respectively. They are to be compared with the current values of (2.7 ± 0.7) × 10^3, 17 ± 4, and 1.2 ± 0.3. With the exception of the results for the CH_3O^- reaction, the agreement is within the experimental uncertainties of the two sets of measurements. The early results (15) for the reactions of CH_3O^- with the allene and toluene, which provided limiting values for K of $\lesssim$ 0.5 and $\lesssim$ 1 respectively, are also superseded by the present measurements, which yielded a value for K of 1.4 ± 0.3 for both of these reactions.

Table 3 provides a comparison of our present and some earlier flowing afterglow results with those obtained by McIver and his colleagues with the pulsed-ICR mass spectrometer which operates at considerably different conditions of total pressure and reagent ion history, and a neutral gas and ion temperature which has been estimated to be 320 K (16). The agreement with the most recent ICR results reduced to apply at a temperature of 298 K (16) is within a factor of 2 in the majority of cases.

Absolute and relative gas-phase acidities

Bartmess and co-workers have recommended an absolute gas-phase acidity for methanol of 372.6 kcal mol^{-1} (16) based on a standard enthalpy change and standard entropy change for the deprotonation of methanol of 379.2 kcal mol^{-1} and 22.0 cal mol^{-1} K^{-1}, respectively. In the same paper these authors have shown that the standard enthalpy change which can be derived from the best available values for EA(CH_3O), D(CH_3O—H), and IP(H) has an average value of 381.2 kcal mol^{-1}. We have adopted this latter value for the standard enthalpy change and recommend an absolute gas-phase acidity for methanol of 374.6 ± 2 kcal mol^{-1}. This value has been used as a reference for the assignment of the absolute gas-phase acidities indicated in Table 4 which also includes the differences in gas-phase acidity determined from the equilibrium constants measured with the flowing afterglow technique.

C. Influence of solvation on intrinsic kinetics and energetics

Under our experimental operating conditions methanol solvent is added as a vapour in trace amounts (< 1%) to a flowing plasma of helium or hydrogen at low total presures (ca. 0.3 Torr). The reagent base, $B^- = CH_3O^-$, is produced by the ionization of methanol and allowed to build up a solvation shell upstream by successive methanol addition reactions to form ions of the type $CH_3O^-.(CH_3OH)_n$. These solvated ions then participate in reactions with the added acid, AH, as they enter the reaction region downstream. An ensuing solvated proton-transfer reaction of type

TABLE 3. A comparison of values for equilibrium constants determined using the flowing afterglow (FA) technique with values determined using the ICR technique

Reaction	K(FA)[a]	K(ICR)[a,b]
$CH_3O^- + C_6H_5CH_3 \rightleftharpoons C_6H_5CH_2^- + CH_3OH$	*1.4 ± 0.3*	*1.7*
$CH_3O^- + C_2H_5OH \rightleftharpoons C_2H_5O^- + CH_3OH$	$(1.6\pm0.7) \times 10^2$ [2]	*1.9×10^2, (23 ± 2)*
$CH_3O^- + C_2H_2 \rightleftharpoons C_2H^- + CH_3OH$	*$(2.7\pm0.7) \times 10^3$*	1.1×10^4 [2], ($(2.9\pm1.2) \times 10^2$ [3])
$C_2H_5O^- + C_2H_2 \rightleftharpoons C_2H^- + C_2H_5OH$	*17 ± 4*	*58* (12 ± 2 [2])
$(CH_3)_2CHO^- + C_2H_2 \rightleftharpoons C_2H^- + (CH_3)_2CHOH$	*1.2 ± 0.3*	*1.2* (1.3 ± 0.1 [2])
$C_2H^- + CH_3CN \rightleftharpoons CH_2CN^- + C_2H_2$	*$(3.0\pm0.7) \times 10^2$*	96 [3]
$CH_2CN^- + CH_3COCH_3 \rightleftharpoons CH_3COCH_2^- + CH_3CN$	*$\geq 5 \times 10^2$*	2.2×10^2 [2]
$CH_3S^- + CH_3NO_2 \rightleftharpoons CH_2NO_2^- + CH_3SH$	*1.9 ± 0.3*[c]	*3.3*
$SH^- + HCN \rightleftharpoons CN^- + H_2S$	*1.6 ± 2*[d]	*6.4, 9.5 ± 1.5*[e]
$CH_3O^-.CH_3OH + C_2H_5OH \rightleftharpoons C_2H_5O^-.CH_3OH + CH_3OH$	*7.7 ± 2.2*	*7.5 ± 2*[f]
$C_2H_5O^-.CH_3OH + C_2H_5OH \rightleftharpoons C_2H_5O^-.C_2H_5OH + CH_3OH$	*2.3 ± 0.6*	*2 ± 0.5*[f]

[a] A value is in italics if the equilibrium has been studied directly. The other values were obtained by combining the results of equilibrium measurements for two or more reactions, the actual number of reactions is given in brackets.

[b] Values of K derived from the values of $\delta\Delta G^0$ (reduced to 298 K) reported by Bartmess, Scott, and McIver in ref. 16 (Fig. 3) unless indicated otherwise. The values in parentheses are those reported earlier by McIver and Miller in ref. 17.

[c] Reference 10.

[d] Reference 18.

[e] Reference 19.

[f] Reference 20.

TABLE 4. Relative and absolute gas-phase acidities at 298 K, ΔGA and GA(AH) in kcal mol^{-1}, based on flowing afterglow measurements. The values in parentheses are those recommended by Bartmess, Scott, and McIver on the basis of pulsed-ICR mass spectrometer measurements (16)

GA(AH)	AH	ΔGA
(345.8)	HCN	
(347.1)	H_2S	1.6 ± 0.1 (1.3)
(352.0)	CH_3NO_2	
(352.7)	CH_3SH	0.4 ± 0.1 (0.7)
≤362.8 (361.6)	CH_3COCH_3	
366.5 (364.4)	CH_3CN	>3.7 (2.8)
369.9 (367.2)	C_2H_2	3.4 ± 0.2 (2.8)
370.0 (367.5)	$(CH_3)_2CHO$	0.11 ± 0.15 (0.3)
371.6 (369.5)	C_2H_5OH	1.7 ± 0.2 (2.3)
374.4 (372.3)	$C_6H_5CH_3$ $CH_2{=}C{=}CH_2$	4.5 ± 0.2 (5.1)
374.6 (372.6)	CH_3OH	0.20 ± 0.13 (0.3) 4.7 ± 0.2 (5.4)

[2] may then establish the newly solvated species $A^-.(CH_3OH)_n$. In the time available in the reaction region these species in turn may optimize their stability by exchanging the methanol molecules in the solvation shell for the acid molecules, AH, or simply by adding the latter. Figure 8 shows a general scheme of the sequential solvated-ion chemistry which is implied by our measurements.

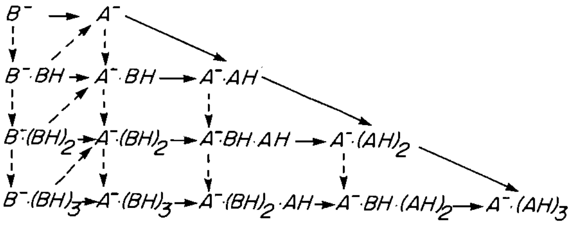

FIG. 8. A general scheme representative of the possible solvated ion chemistry proceeding under flowing afterglow conditions. The solid horizontal arrows represent solvated acid–base or solvent exchange reactions with AH. The solid diagonal arrows represent solvent addition reactions with AH. The dashed vertical arrows represent possible solvent addition reactions with BH. The dashed diagonol arrows represent possible solvated acid–base reactions with a concomitant "boiling off" of solvent BH.

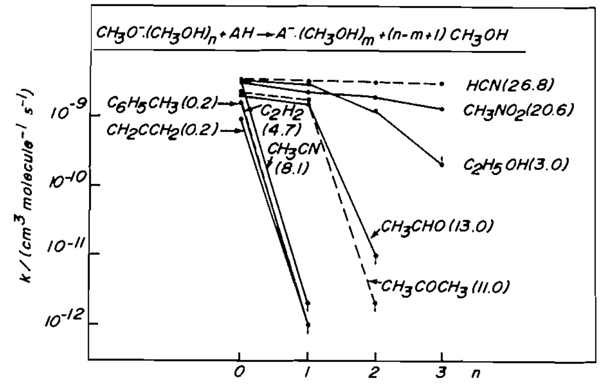

FIG. 9. Observed variations in the rate constants for the reactions of solvated methoxide ions with acids AH as a function of step-wise solvation. The values indicated in parentheses correspond to the relative intrinsic acidities of the acids AH and CH_3OH, i.e. $-\Delta G^0$ (in kcal mol^{-1}) for the solvent-free reactions at 298 K.

The chemical sequence indicated may be interrupted at any level of solvation depending on the nature of the added acid.

The rate constants obtained for the solvated proton-transfer reactions of the species $CH_3O^-.(CH_3OH)_2$ with the acids added in this study are summarized in Table 2 and presented graphically in Fig. 9. Solvation of CH_3O^- is seen to lead to two extreme types of behaviour: (*a*) The addition of only one methanol molecule to the methoxide ion essentially closes the reactions of this ion with allene, toluene, acetylene, and methylcyanide. The rate constant is observed to drop dramatically by more than a factor of ~ 10^3 from an initial value of ca. 10^{-9} cm^3 $molecule^{-1}$ s^{-1}. (*b*) For the reactions of ethanol, nitromethane, and hydrogen cyanide the addition of three molecules of methanol does not reduce the rate by more than a factor of ~ 10. The reactions with acetone and acetaldehyde show an intermediate behaviour in that the sharp drop in rate is delayed until the addition of two molecules of methanol to the methoxide ion.

The remarkable divergence of the rate constants observed in this study can be accounted for by a consideration of the degree of stabilization of the reactant and product ions by solvation and their influence on overall reaction energetics. The rate of proton transfer can be expected to remain high upon solvation if the reaction remains exoergic. Conversely, a sharp drop in the rate can be anticipated if solvation renders the reaction endoergic. The solvent-free reactions are all exoergic: they span a range in $-\Delta G^0$, i.e. relative intrinsic acidity, from 0.2 to 26.8 kcal mol^{-1}. The free energy of solvation of CH_3O^-, which can be deduced to be approximately 17 kcal mol^{-1} for the addition of the first methanol molecule (1), will act to decrease the reaction exoergicities and can lead to changes in the sign of ΔG^0, i.e. reversals in relative acidity, and therefore reversals in the preferred direction of reaction unless it is offset by the solvation energy of the conjugate base produced. In other words, exoergicity will be preserved if the free energy of solvation of the conjugate base produced is comparable to or greater than the corresponding free energy of solvation of CH_3O^- or if a lower free energy of solvation of the product base is offset by the exoergicity of the unsolvated reaction.

The carbanions produced by the deprotonation of allene and toluene, the two acids in this study with an intrinsic acidity almost identical to that of methanol, are expected to have free energies of solvation insufficient to compensate for the high solvation energy of CH_3O^-. The sharp drop in the rate of deprotonation observed upon the addition of just one molecule of solvent can therefore be interpreted as a manifestation of a reversal in the relative acidity of these two carbon acids and methanol. A similar situation seems to apply to the formation of $C_2H^-.CH_3OH$ and $CH_2CN^-.CH_3OH$ although the solvent-free reactions are somewhat more exoergic. Again a reversal in relative acidity appears to result after the addition of just one methanol molecule.

For the deprotonation of acetone and acetaldehyde by CH_3O^- reversals also appear to occur but they are delayed by one additional molecule of solvent: the sharp decline in rate occurs at $n = 2$. In these cases the exoergicities of the solvent-free reactions are within 6 kcal mol^{-1} of compensating for the high free energy of solvation of CH_3O^-. Also some of the negative charge on the anions produced from these two carbon acids is transferred to the oxygen which may result in some enhancement in the stability of the solvated species.

No reversals are observed for the deprotonation of nitromethane, hydrogen cyanide, and ethanol: reaction [2] remains rapid up to the addition of three methanol molecules to CH_3O^-. The intrinsic acidity of ethanol, an oxygen acid, is relatively close to that of methanol but in this case the order of acidity is preserved by the strong solvation of $C_2H_5O^-$. The intrinsic acidities of nitromethane and hydrogen cyanide are sufficiently high to offset the weaker anion–methanol interactions expected for $CH_2NO_2^-$ and CN^-. In fact, reactions of type [37] for AH = HCN or CH_3NO_2 in which some of

$$[37]\quad CH_3O^-.(CH_3OH)_n + AH \rightarrow A^-.(CH_3OH)_m + (n - m + 1)CH_3OH$$

the methanol is "boiled off" are exoergic at least for $n = 1$ and $m = 0$. Indeed the product spectra observed for these two reactions appear to be "shifted" in favour of lower degrees of solvation of A^-.

The clear pattern which has emerged from the trends in the rates of the acid–base reactions of the solvated methoxide ions which have been determined in this study and their dependence on the overall energetics of reaction is likely to be representative of the transition from the gas-phase to the solution in the rates of exothermic acid–base reactions generally and provides a vivid confirmation of expectations based on solution measurements.

Acknowledgement

We thank the Natural Sciences and Engineering Research Council for financial support. Also we thank one of the referees for drawing our attention to the possibility of aldol-type condensations for several of the association reactions observed in this study.

1. G. I. MACKAY and D. K. BOHME. J. Am. Chem. Soc. **100**, 327 (1978).
2. S. D. TANNER, G. I. MACKAY, and D. K. BOHME. Can. J. Chem. **59**, 1615 (1981).
3. D. K. BOHME, R. S. HEMSWORTH, H. W. RUNDLE, and H. I. SCHIFF. J. Chem. Phys. **58**, 3504 (1973).
4. G. I. MACKAY, R. S. HEMSWORTH, and D. K. BOHME. Can. J. Chem. **54**, 1624 (1976).
5. G. I. MACKAY and D. K. BOHME. Org. Mass. Spectrom. **15**, 593 (1980).
6. A. C. HOPKINSON. *In* The chemistry of functional groups. The chemistry of the carbon–carbon double bond. *Edited by* S. Patai. John Wiley and Sons, Toronto. 1978. Chapt. 4, p. 85.
7. G. I. MACKAY, K. TANAKA, and D. K. BOHME. Int. J. Mass Spectrom. Ion Phys. **24**, 125 (1977).
8. G. I. MACKAY, L. D. BETOWSKI, J. D. PAYZANT, H. I. SCHIFF, and D. K. BOHME. J. Phys. Chem. **80**, 2919 (1976).
9. D. K. BOHME, G. I. MACKAY, H. I. SCHIFF, and R. S. HEMSWORTH. J. Chem. Phys. **61**, 2175 (1974).
10. G. I. MACKAY and D. K. BOHME. Int. J. Mass Spectrom. Ion Phys. **26**, 327 (1978).
11. T. SU, E. C. F. SU, and M. T. BOWERS. J. Chem. Phys. **69**, 2243 (1978).
12. C. LIFSHITZ, R. L. C. WU, and T. O. TIERNAN. J. Am. Chem. Soc. **100**, 2040 (1978).
13. J. I. BRAUMAN, C. A. LIEDER, and M. J. WHITE. J. Am. Chem. Soc. **95**, 927 (1973).
14. D. K. BOHME, E. LEE-RUFF, and L. B. YOUNG. J. Am. Chem. Soc. **93**, 4608 (1971).
15. D. K. BOHME, E. LEE-RUFF, and L. B. YOUNG. J. Am. Chem. Soc. **94**, 5153 (1972).
16. J. E. BARTMESS, J. A. SCOTT, and R. T. MCIVER. J. Am. Chem. Soc. **101**, 6046 (1979).
17. R. T. MCIVER and J. S. MILLER. J. Am. Chem. Soc. **96**, 4323 (1974).
18. D. BETOWSKI, G. I. MACKAY, J. PAYZANT, and D. K. BOHME. Can. J. Chem. **53**, 2365 (1975).
19. R. T. MCIVER, JR. and J. R. EYLER. J. Am. Chem. Soc. **93**, 6334 (1971).
20. R. T. MCIVER, JR., J. A. SCOTT, and J. M. RIVEROS. J. Am. Chem. Soc. **95**, 2706 (1973).